Performance analysis of a heat pump with desuperheater for residential buildings using different control and implementation strategies

F. Hengel*, A. Heinz, R. Rieberer

Institute of Thermal Engineering, Graz University of Technology, Inffeldgasse 25/B, A-8010 Graz, Austria

This is an author-produced version of a paper accepted for publication in the Applied Thermal Engineering journal (Elsevier) in May 2016. This version has been peer-reviewed, but does not include the final publisher proof corrections, published layout, or pagination.
For the official version, please refer to doi:
http://dx.doi.org/10.1016/j.applthermaleng.2016.05.110

Abstract

In this study, an extensive analysis of a desuperheater (DES) applied in a combined solar and air-source heat pump (ASHP) system for a residential low heating energy building (45 kWh/(m²a)) is carried out using the climatic conditions of Graz. The heat pump system uses R410A as refrigerant and has a heating capacity of 4.9 kW (@ A-12W35). The main focus of the investigation lies on the analysis of five different control strategies and types of integration of the DES into the system. For the investigations a validated TRNSYS heat pump model is implemented into a system simulation model, which comprises a buffer storage, a thermal solar collector and the heat distribution and heat dissipation system.

The results show energy saving potentials by applying a DES compared to the reference system without DES. This is mainly due to the lower amount of heat provided for “direct” domestic hot water (DHW) preparation by the heat pump. The results for the investigated control strategies show a maximum increase of the seasonal performance factor (SPF) and electrical energy savings of 5.3 % and 5.0 %, respectively, for an extra hydraulic loop of the DES with its own circulation pump. The other four strategies show annual electrical energy savings of about 4 % compared to the reference system without DES.

Keywords: air-to-water heat pump; desuperheater; heat pump model; combined solar and heat pump

* Corresponding author. Tel.: +43 316 873 7301
E-Mail address: office.iwt@tugraz.at

Nomenclature		Greek symbols	
ASHP	Air-source heat pump	τ	Time in s
BUI	Building	λ	Thermal conductivity in W/(mK)
c	Specific heat capacity	π	Pressure ratio
Cdot	Capacity flow ($\dot{m} \cdot c_p$) in W/K		
COP	Coefficient of performance		
DHW	Domestic hot water	Subscripts	
DES	Desuperheater	amb	Ambient
f	Factor	$comp$	Compressor
GSHP	Ground-source heat pump	$cond$	Condenser
HP	Heat pump	ctr	Control devices
$\dot{m}$	Mass flow rate kg/h	DHW	Domestic hot water
Mfr	Mass flow rate in kg/h	DES	Desuperheater
P	Power in kW	el	Electric
$\dot{Q}$	Heating capacity in kW	hp	Heat pump or high pressure
Q	Energy in kWh	in	Inlet
REF	Reference system (without DES)	out	Outlet
RIP	Relative inlet position	pen	Penalty
ROP	Relative Outlet position	pu	Circulation pump
SC	Solar Collector loop	ref/r	Refrigerant
SH	Space heating	sc	Solar collector loop
SPF	Seasonal Performance Factor	set	Set point
T	Temperature in K	SH	Space heating
TES	Thermal energy storage	sub	Diff. between discharge temperature and DES water outlet temperature
ΔT	Temperature difference in K	sys	System
var	Variable	th	Thermal Energy in kWh_{th}
W	Work in kJ or kWh or MWh	w	Water

1 Introduction

Heat pumps are widely used for domestic hot water (DHW) preparation and space heating (SH) and offer the possibility to substitute conventional heating systems (direct electric, oil boiler, gas boiler etc.) and to reduce the primary energy consumption [1].

Especially air-source heat pumps (ASHP) are widely used in residential heating and cooling systems due to their low installation costs and their effectiveness [2]. The European heat pump market shows that air-to-water heat pumps play an important role, reflected in their large market share [3]. The Austrian heat pump market has also developed towards an increase of air-to-water heat pumps in the recent decade [4].

Concerning the increasing market share of ASHPs it is of interest to increase the performance of this technology. One possibility is to implement a desuperheater (DES), which is an additional small heat exchanger that is installed directly after the compressor and before the actual condenser of the heat pump. The DES transfers the heat of the superheated refrigerant vapor to a secondary circuit, which is connected to a thermal energy storage (TES) system, where the energy can be stored and then used for DHW (directly or indirectly). The condensation of the de-superheated refrigerant takes place in the condenser of the heat pump, which usually transfers heat to the heating system or to a buffer storage tank. Hence heat pump operation with a DES usually means a simultaneous preparation of heating water for space heating with a moderate temperature (30 to 35 °C in case of a floor heating system) and DHW with a relatively high temperature of 50 to 60 °C. The advantage of this simultaneous operation is that the heat pump operates at a lower high-side pressure compared to DHW preparation only.

Experimental investigations concerning the thermal performance of a DES for DHW preparation analyzing the effect of different water and refrigerant inlet temperatures have been performed by Lee & Jones [5] and they used the data to validate an analytical model [6]. Shao et al. [7] have done a simulation study using a desuperheater and a preheater for DHW for different modes of heating and cooling operation in an air-to-water system. They are reporting energy savings of 31%, which are achieved compared to a system using direct electrical water heating.

A ground-source heat pump system (water-to-water) used for heating and cooling, equipped with a desuperheater for DHW preparation was investigated by Cui et al. [8] by means of simulations. The system was compared to a conventional ground-coupled heat pump system, also using an electric heater for preparing DHW. However, nearly 95% of the DHW demand can be covered by the desuperheater system. Biaou and Bernier [9] have studied four systems for preparing DHW, including a ground-source heat pump with a desuperheater. Also here a direct comparison between DHW preparation by a heat pump with and without desuperheater was not performed.

The natural refrigerant ammonia in a low capacity heat pump system with DES has been investigated by Palm [10] by means of laboratory tests. The results within this study show high COP values. However, some problems concerning the lack of available components for ammonia, like a hermetic compressor for ammonia and problems due to poor lubrication are also reported.

A validated GSHP heat pump model with DES has been developed by Blanco et al. [11]. The authors used the COP as key parameter for the evaluations and stated that the highest COP for space heating (SH) mode and combined SH and DHW preparation occur at different superheating degrees. An analysis of the annual performance of a heat pump system with desuperheater was not performed. In [12] the same authors have done experimental investigations on a monovalent inverter-driven water-to-water heat pump. Three modes (SH heating only, DHW preparation only and combined mode) have been examined, where the coefficient of performance was used as key parameter. An analysis of the annual performance and a comparison to a system without desuperheater was not performed. In [13] the same authors have performed investigations of the seasonal performance of a monovalent inverter-driven water-to-water heat pump with a desuperheater by means of simulations. However, the focus of this study was on control schemes for different electricity tariff plans in order to minimize costs.

Among the more recent work is Safa et al. [14]. Here a field test study in two buildings has been carried out under the climatic conditions of Ontario. The obtained and extrapolated measured results indicate a potential to increase the system efficiency by implementing a DES in GSHPs. Also recent research work on hybrid renewable microgeneration system for multiple residential and small office buildings by means of TRNSYS simulations has been done by Entchev et al. [15]. Within this study three cases were investigated where a conventional system (boiler) was used as reference case and compared to two GSHP systems (with and without photovoltaic thermal collector) including a DES for DHW. The results show high potential to save overall energy by applying renewable systems including DES for DHW in multiple residential and small office buildings. Within this study the DES is implemented in the overall renewable system but not analyzed in detail.

Liu et al. [16] have done an experimental study of a multifunctional water source heat pump system with desuperheater, where in the heating mode, hot water is produced by two-step heating (two heat exchangers, DES and condenser). Results are based on experiments and an analysis of the seasonal performance is not reported.

A system, in which the heat pump condenser and desuperheater are integrated into a storage tank, was presented by Heinz et al. [17]. A simulation model for the system has been developed and validated with experimental data. An analysis of the seasonal performance of the system was not yet reported.

Although in literature different studies concerning the use of a DES in heat pump systems can be found, dealing with both the analysis of the refrigerant cycle and the effect on the overall system performance, a detailed direct comparison of the annual performance of an ASHP with and without a DES for DHW preparation under the same boundary conditions cannot be found. Publications on the use of a DES in combined solar and heat pump systems are also not available so far.

Based on the literature survey and the increasing market share of ASHP's the aim of this paper is to investigate a DES applied in an ASHP in a combined solar heat pump system. Within this work different options of the system integration and control strategies of the DES are analyzed and the SPF as well as the electrical energy savings are used as performance figures for the comparison of a heat pump with and without a DES.

2 Heat pump model

2.1 Description

The simulation was performed by means of dynamic system simulations in TRNSYS [18] using the semi-physical heat pump model Type 877 [19]. The model is based on the refrigerant cycle using the thermodynamic properties of the refrigerant. The modeling of the compressor efficiency is done by using the overall isentropic efficiency $\eta_{is,over}$ and the volumetric efficiency η_{vol}, both depending on the condensation and evaporation temperatures. The heat exchangers are modeled using UA-values, which are adapted depending on the mass flow rates on both sides, and the conditions at the inlet of the heat exchanger (mass flow rate, pressure, temperature). Figure 1 shows on the left side the heat pump cycle with its components like compressor, desuperheater (DES), condenser, expansion device and the air-source evaporator. The corresponding temperature-enthalpy-diagram is depicted on the right side. A more detailed description of the heat pump model and a comparison with measured data can be found in [19].

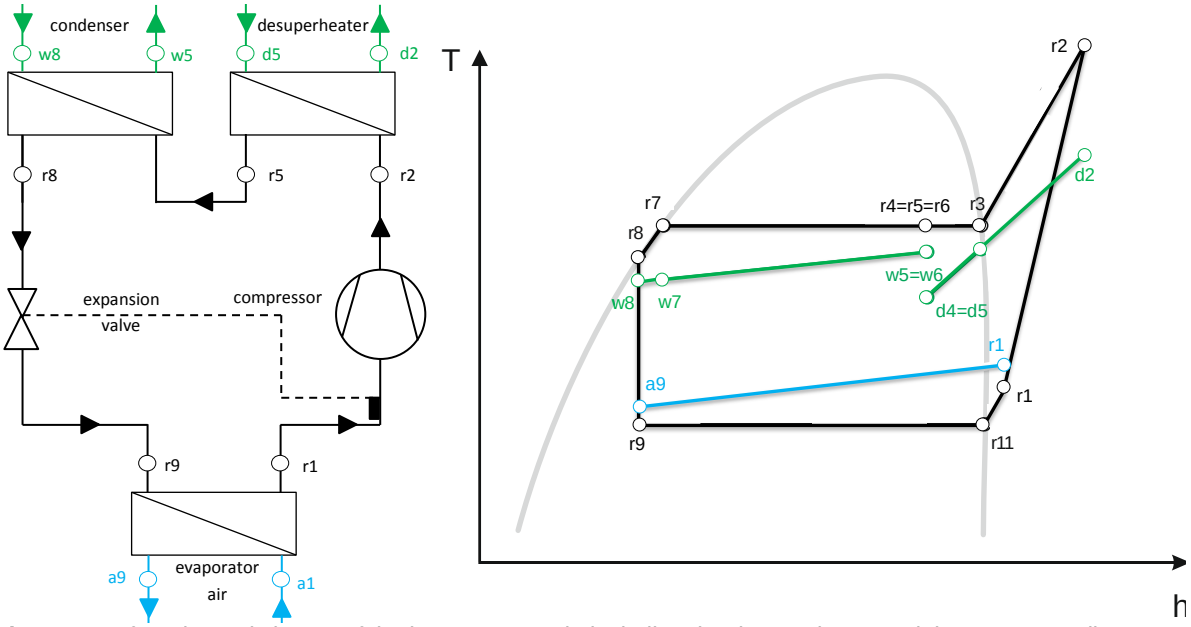

Figure 1: Left: Schematic layout of the heat pump cycle including the desuperheater; Right: Corresponding exemplary process in the temperature-enthalpy-diagram (T-h-diagram) with all heat exchangers active [19]

2.2 Assumptions

Since the focus for the simulations lies on the investigations of the DES, a single speed compressor is assumed, using a performance map generated from manufacturer data [20]. With the compressor chosen the heat pump is able to cover the heat load of the building at the design ambient temperature (3.74 kW @ -12 °C) without any backup system.

Due to the relatively high variation of the mass flow rates on both sides (refrigerant and the secondary side, water or air) the UA-values of the heat exchangers are varied depending on the flow rates. For this purpose polynomial functions for the UA-values of condenser and DES (except evaporator) were set-up based on measurements from a brine-to-water heat pump prototype built in the laboratory of the Institute of Thermal Engineering. The UA-values for the air-source evaporator are based on manufacturer data. The superheating at the outlet of the evaporator is assumed to be at constantly 5 K (e.g. controlled by an electronic expansion valve).

The electrical power consumption of the evaporator fan is also based on manufacturer data. The nominal electrical power consumption of the fan is 120 W at a speed of 650 rpm at ambient temperatures below 15 °C. The speed of the fan is constant below an ambient temperature of 15 °C and is linearly reduced above (0 rpm @ 45 °C) in order to stay within the compressor's operational limits (max. evaporation temperature).

A simplification of the heat pump model is that the heat losses of the refrigerant cycle (except the heat losses of the compressor) as well as the pressure drop in pipes and heat exchangers are neglected. The start and stop losses are calculated in a simplified way with an exponential function and a time constant. The defrosting losses are considered in a steady-state manner by estimating a growth of ice on the evaporator depending on the evaporation temperature and the temperature and humidity of the ambient air. The estimated heating capacity, which is necessary for melting the ice on the evaporator, is subtracted from the capacity of the condenser, thus reducing the COP.

The heat pump model with DES has been validated with data from a heat pump prototype built in the laboratory, as published in Hengel et al. [21].

3 System description and boundary conditions

3.1 Overall system

The heat pump described in chapter 2 is implemented into a system to evaluate the performance of the DES by means of simulations, whereby R410A is chosen as refrigerant. Figure 2 shows the combined solar heat pump system, as described in Bales et al. [22], which is used as reference system. The main components are the ASHP, the thermal energy storage (TES), the solar collector loop, the building and its heating system and the DHW tapping integration.

The system layout, which was defined in the European project MacSheep, is based on systems that are currently suggested and promoted by leading companies in the heating sector in Europe. Herein a water storage tank is used, which can be charged in parallel from the solar collector loop and the heat pump system. Both the solar charging (with T_{SC} as temperature sensor) and the DHW preparation (T_{DHW}) are integrated into the TES via internal heat exchangers. The storage is filled with the same water as the heating system, which is separated from the DHW by the DHW heat exchanger. The solar collector loop uses a glycol/water (35%/65%) mixture to prevent freezing at low ambient temperatures. The heat pump is connected to the store via three pipes, which can be used like four connections. The upper two pipes are used for charging the upper part of the TES, which is used for DHW preparation. For charging the volume for space heating (T_{SH}), which is located in the middle part of the TES, the connection can be switched via two 3-way-valves, in order to connect the supply line of the heat pump to the middle port and the return to the lowest of the three ports. The supply line of the space heat distribution system is also directly connected to the middle port and the return to the lowest port. When the store is being charged for space heating, some of the flow will pass via the space heating distribution loop and the rest will pass through the store. The exact proportions depend on the operating conditions of the space heating distribution loop (that has a thermostatic valve) and on the flow temperature from the heat pump. The control strategies of the overall system as well as the heat pump are the same as published in [22]. The mass flow rate over the condenser is set in order to reach a temperature difference of 5 K at design ambient conditions.

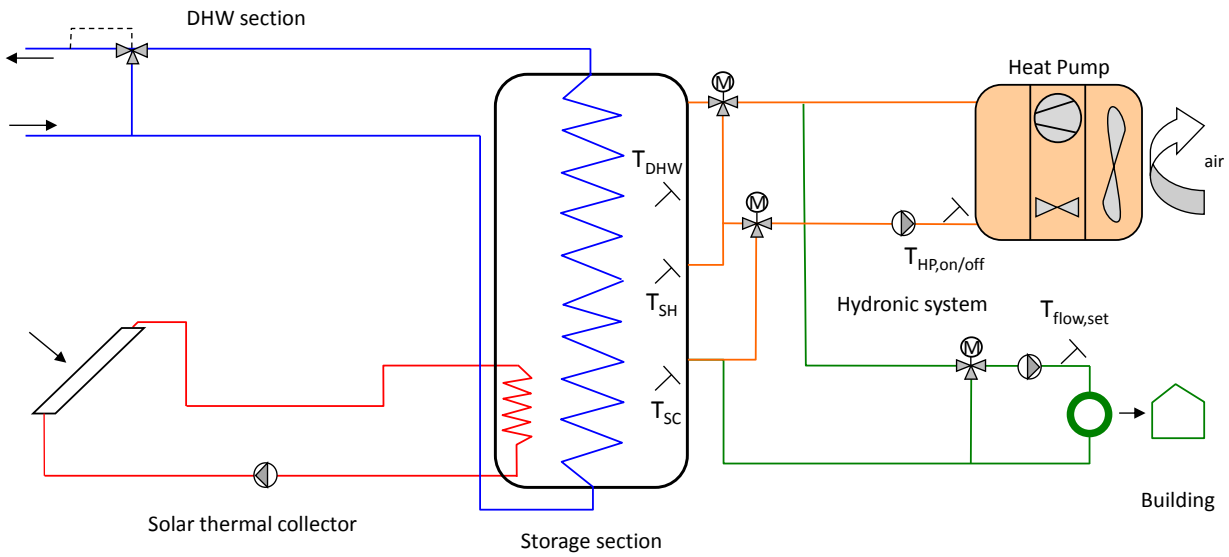

Figure 2: Schematic of the combined thermal solar collector and air source reference system with its temperature sensors for charging the storage (T_{DHW}, T_{SH}, T_{SC}) and to control the heat pump ($T_{HP,on/off}$) as well as flow temperature to the heating system ($T_{flow,set}$) [22]

Table 1 contains the main TRNSYS simulation models, references to the model documentations and the most important parameters.

Table 1: Most important information concerning the reference system with used models within the simulation environment, references and parameter settings

Model	TRNSYS Type number	Type Documentation	Parameter / Description
Solar Collector / loop (SC)	T832v500	[23]	glazed collector: $\eta_0 = 0.793$, $a_1 = 3.95$ W/(m²K), $a_2 = 0.0122$ W/(m²K²); inclination: 45°; orientation: south; 9.28 m² heat exchanger UA-value: 312.5 W/(m²K)
Thermal Energy Storage (TES)	T340	[24]	Buffer storage; volume: 0.763 m³, height: 1.74 m; DHW heat exchanger UA-value: 368 W/(m²K) HP to TES for DHW, relative inlet position (RIP): 1.0, relative outlet Position (ROP): 0.49; HP to TES for SH, RIP: 0.49; ROP: 0.26 TES to Building (BUI), RIP: 0.26, ROP: 0.49 SC to TES: RIP: 0.45, ROP: 0.0 TES to DHW discharge: RIP: 0.03, ROP: 0.95 relative sensor positions: Temperature DHW (T_{DHW}): 0.65 Temperature SH (T_{SH}): 0.44 Temperature SC (T_{SC}): 0.18
Heat Pump (HP)	T877	[19]	Air HP with scroll compressor: Heating Capacity @A-12W35: 4.85 kW, COP: 2.85 Heating Capacity @A2W35: 7.25 kW, COP: 4.21
Building	T56	[25]	standard type; detailed information in 3.2

3.2 Climate and building

A climate data set of Graz[1] is chosen with a design ambient air temperature of -12 °C and heating degree days of 3102 Kd/a. The calculation is done with a room temperature of 20 °C.

The assumed building is the reference building from the IEA SHC TASK 44/HPP ANNEX 38 (T44A38) [26], which has a heated floor area of 140 m² and a heating demand of 45 kWh/(m²·a) for the climate Strasbourg. For the climate Graz the heating demand is a bit higher with 46.3 kWh/(m²·a).

With an indoor temperature of 20 °C the design load for heat distribution of the considered building is 3.74 kW. The supply temperature of the applied floor heating system is 35 °C and the return temperature is 30 °C at design ambient conditions with a radiator exponent of 1.1. The chosen heat pump has a heating capacity of 4.85 kW and is thus slightly oversized. As a fraction of the heating capacity is used by the desuperheater to charge the upper part of the store (compare section 3.3), it should be ensured that enough capacity is available at the condenser. To satisfy the comfort level in the building a penalty function is implemented in the calculation of the seasonal performance factor SPF (equation (3)), which must not exceed 1 % of the space heating demand [27].

For the DHW draw-off profile a data set from the project MacSheep is used [22]. The annual DHW heat demand with a temperature difference of 35 K (45 °C DHW temperature and 10 °C cold water temperature) is 2913 kWh/a, which represents the demand for four persons. Similar as for space heating a penalty function is implemented (equation (3)), which must not exceed 1 % of the DHW demand. A description of the used penalty functions for space heating and DHW can be found in [27]. All simulations with a penalty greater than this are deemed not to fulfil the comfort requirements and are excluded from evaluation.

3.3 Desuperheater system integration and control strategies

This subchapter describes the control strategies and types of implementation of the DES in the overall system (Table 2) are investigated in this work.

For all strategies the DES is used in series to the condenser (on the refrigerant side) to charge the upper part of the TES. Simultaneous preparation of DHW with the DES is always done, when the heat pump is running in space heating mode. If T_{DHW} is lower than 48 °C, the system switches to DHW preparation only mode until T_{DHW} reaches 52 °C. In heating mode the heat pump is started, when T_{SH} drops below $T_{flow,set}$ minus a hysteresis of 3 K. The heat pump is stopped, when $T_{HP,on/off}$ reaches $T_{flow,set}$. If the TES is sufficiently charged, space heating is done out of the TES and the heat pump is off.

The first four strategies use the hydraulic layout shown in Figure 3, where a part of the total water mass flow rate (from the condenser) is split at the outlet of the condenser and passes the DES. The amount of water mass flow rate passing the DES depends on the used control strategy and is controlled by the 3-way-valve. During direct DHW preparation the DES is used in series to the condenser (on the water side) with the 3-way-valve fully opened (same water mass flow through the condenser and the DES).

In strategy 1 the 3-way-valve controls the mass flow rate through the DES in a way to reach the set point temperature (e.g. $T_{DES,set}$ = 57 °C). If the compressor discharge temperature is too low, $T_{DES,set}$ is reduced to the discharge temperature minus 1.5 K within the heat pump model.

Strategy 2 uses the 3-way-valve to set a defined temperature difference (e.g. ΔT_{comp} = 2 K) between the compressor discharge temperature and the water outlet temperature at the DES.

The third strategy also uses the 3-way-valve, but with the difference that the opening degree is constant, assuming a constant mass flow. In strategy 4 the control valve sets the water mass flow

[1] Based on monthly data (average monthly data of the years 2001 – 2010), hourly values of all parameters were calculated with the Software METEONORM. The resulting time series represents a “typical year” at the considered location

rate through the DES in a way to reach the same capacity flow rate ($\dot{m} \cdot c_p$) on the refrigerant and the water side.

Table 2: Definition of the implemented DES strategies

No.	Description	Parameter
1	Use of a fixed water temperature at the outlet of the DES	$T_{DES,set}$
2	Use of a fixed temperature difference between the compressor discharge temperature and the water outlet temperature at the DES	ΔT_{comp}
3	Use of a fixed water mass flow rate through the DES	$\dot{m}_{w,DES}$
4	Equal "capacity flow"[2] rates on refrigerant side and water side of the DES	$\dot{C}_{DES}$
5	DES implementation is independent of the condenser with its own circulation pump	$\dot{m}_{DES,ExtraLoop}$

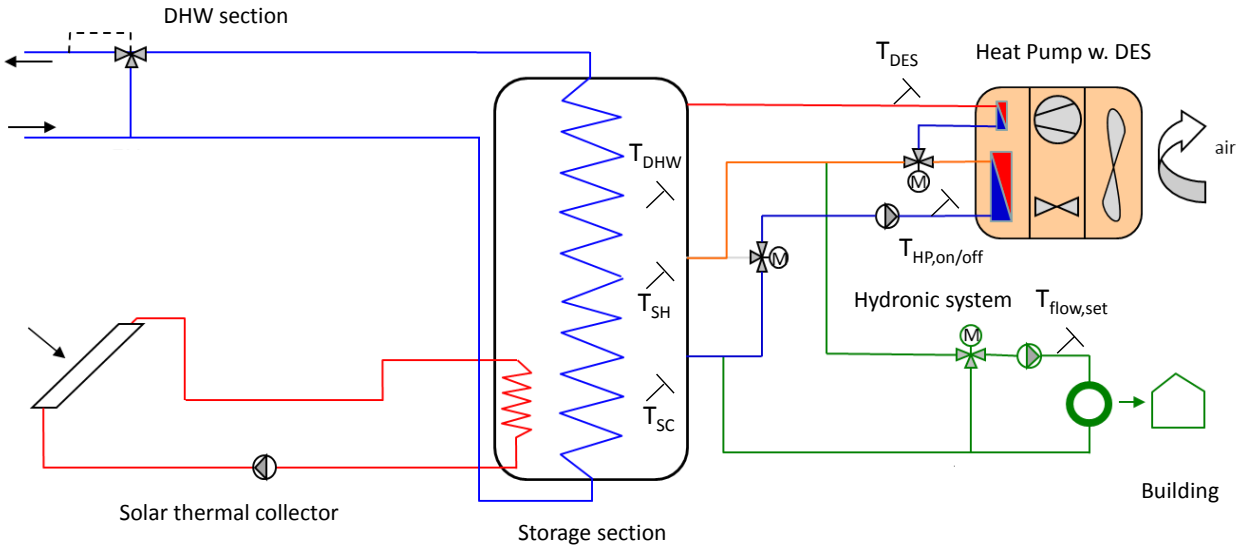

Figure 3: Schematic layout of adapted combined thermal solar and heat pump system by integrating the DES in the hydronic system according to strategy 1 to 4

In strategy 5 an extra loop for the DES is used with its own circulation pump (compare Figure 4). For the circulation pump a high efficiency pump is assumed with a max. electricity consumption of 10 W. Also the pipe dimension of the connections between the store and the DES (length is 6 m) are reduced from an inner diameter of 25 mm to 8 mm because the DHW only mode (with a larger water flow rate) is only done via the condenser. For the reduced pipe diameter the pipe insulation (thermal conductivity is 0.042 W/(mK)) is also reduced from 30 mm to 20 mm. Due to smaller pipe dimensions the heat losses can be reduced. Cooling down of the top of the TES by the DES cannot occur, because if the TES is fully charged, the heat pump is off. If the heat pump is on, the temperature at the middle stage of the TES is lower than the discharge temperature of the compressor.

[2] Capacity flow rate $\dot{C}$ is defined as the product of the mass flow rate $\dot{m}$ and the specific heat capacity c_p

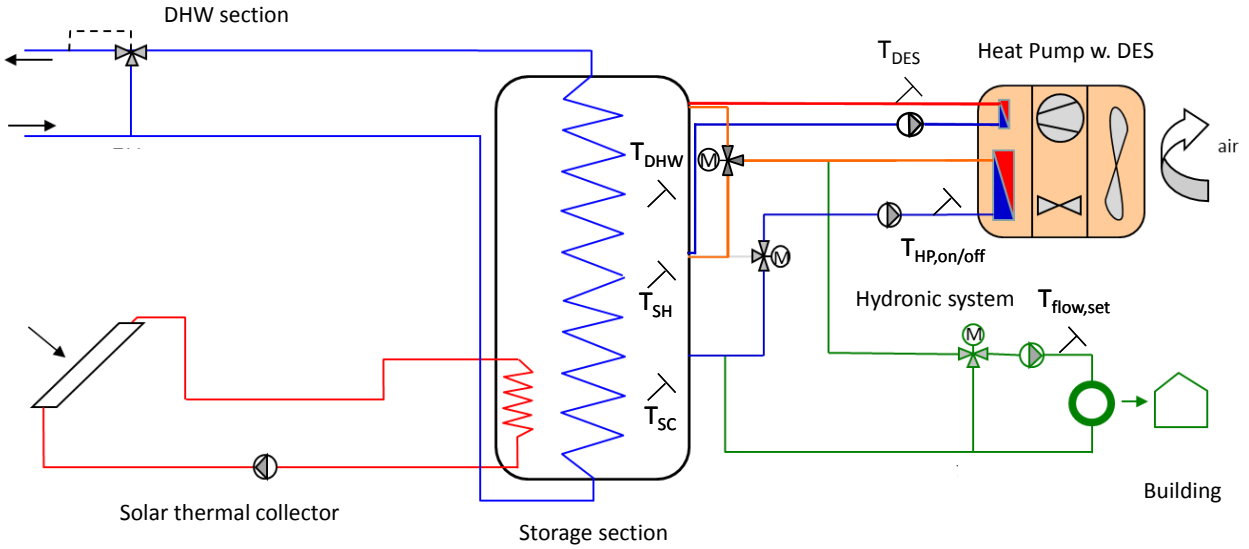

Figure 4: Schematic layout of adapted combined solar and heat pump system by integrating the DES in the hydronic system according to strategy 5

4 Key figures

For the comparison of the different systems the electrical power consumption $P_{el,sys}$, the coefficient of performance (COP) and the seasonal performance factor SPF_{sys} are used, which are defined as follows (eq. (1) to (3)).

$$P_{el,sys} = P_{el,hp} + P_{el,pu} + P_{el,ctr} \tag{1}$$

$$COP = \frac{\dot{Q}_{cond}}{P_{el,hp}} \tag{2}$$

$$SPF_{sys} = \frac{\int_{\tau=0}^{8760h} \left(\dot{Q}_{SH} + \dot{Q}_{DHW}\right) \cdot d\tau}{\int_{\tau=0}^{8760h} \left(P_{el,sys} + P_{el,SH,pen} + P_{el,DHW,pen}\right) \cdot d\tau} \tag{3}$$

$P_{el,sys}$	Electricity consumption of all components (HP, controller, pumps) in kW
$P_{el,hp}$	Electricity consumption of entire HP (compressor, fan, controller) in kW
$P_{el,pu}$	Electricity consumption circulation pumps incl. space heating pump in kW
$P_{el,ctr}$	Electricity consumption of all controllers is 0.02 kW
$\dot{Q}_{cond}$	Heating capacity of the condenser in kW (incl. DES)
$\dot{Q}_{SH}$	Heating capacity space heating in kW
$\dot{Q}_{DHW}$	Heating capacity domestic hot water in kW
$P_{el,SH,pen}$	Penalty space heating in kW [27]
$P_{el,DHW,pen}$	Penalty DHW in kW [27]

5 Results and Discussion

This chapter shows the results of the simulations that were carried out within this work. On the one hand steady-state heat pump cycle simulations were performed, in order to provide a better understanding and a comparison of the different control strategies by illustrating an exemplary operating point in temperature-enthalpy diagrams. On the other hand annual system simulations in TRNSYS were performed, in order to compare the annual performance of the different systems to the reference system. In this context, a variation study was done for each strategy by varying the parameter listed in Table 2, in order to evaluate the influence on the performance.

5.1 Steady-state analysis

Within this subchapter the steady-state results for an exemplary operating point of the ASHP with DES are discussed. The steady-state results are shown in T-h-diagrams in Figure 5 for the different strategies together with the reference system without DES (Ref). For strategy 1 $T_{DES,set}$ is set to 57 °C, for strategy 2 a temperature difference of 2 K between discharge temperature and DES outlet temperature is assumed. For strategy 3 a fixed water flow rate of 30 kg/h over the DES is used. Strategy 4 using equal capacity flow rates on the water and refrigerant side of the DES and strategy 5 with its own DES-loop with a mass flow rate of 30 kg/h and a water inlet temperature of 40 °C into the DES are also shown.

For all strategies the same water mass flow rate through the condenser is assumed ($\dot{m}_{cond,w}$ = 835 kg/h). The UA-values of the condenser and DES are depending on the flow rates on the refrigerant and water sides, as described in chapter 2. For the strategies 1 to 5 the total heat exchanger area on the sink side is about 21 % larger due to the additionally implemented DES.

All five strategies are investigated for an operating condition, which is representative for the operation during a very large part of the heating season (A2W30). Here, the condenser water outlet temperature ($t_{w,cond,out}$) of the reference system is 30 °C. For the systems with DES the heating capacity of the condenser is lower, as a part of the heat rejected at the high pressure side is used for the DES. As the same water flow rate is assumed through the condenser, the water outlet temperature is lower. However, in the system considered here it is assumed that this should not be a problem, as the heat pump is overdimensioned compared to the heat load of the building (compare section 3.2).

The detailed results in Table 3 show that the difference in COP between the investigated strategies 1 to 5 compared to the reference system (Ref) is almost negligible. However, system 4 shows a slightly higher COP, which is due to the lowest temperature difference between the condensation temperature (temperature of saturated vapor on the high pressure side) and the temperature on the water side of the heat exchanger at the same enthalpy (pinch point). Due to the smaller temperature difference in the pinch point a lower condensation temperature occurs.

Another point is that the highest COP is obtained by a heat pump system with DES due to the increased heat exchanger area and in cases where the refrigerant outlet temperature of the DES is closest to the saturated vapor line. In these cases the condensation temperature is slightly lower, i.e. a lower π_{comp}.

Table 3: Detailed results of the steady state investigations at a condition that is representative for the heat pump operation during a very large part of the heating season (A2W30)

Description	$t_{air,in}$ in °C	$t_{w,cond,in}$ in °C	$t_{w,cond,out}$ in °C	$t_{w,DES,out}$ in °C	$t_{r,cond,}$ in °C	$\dot{Q}_{DES}$ in kW	$\dot{Q}_{Cond}$ in kW	COP
Ref	2	23	30.4	-	32.99	-	7.0	4.11
1	2	23	29.3	57.0	32.73	1.0	6.0	4.13
2	2	23	29.7	64.0	32.86	0.7	6.3	4.12
3	2	23	29.4	58.1	32.75	1.0	6.0	4.13
4	2	23	29.2	55.0	32.69	1.1	5.9	4.14
5	2	23	29.7	60.3	32.85	0.7	6.3	4.12

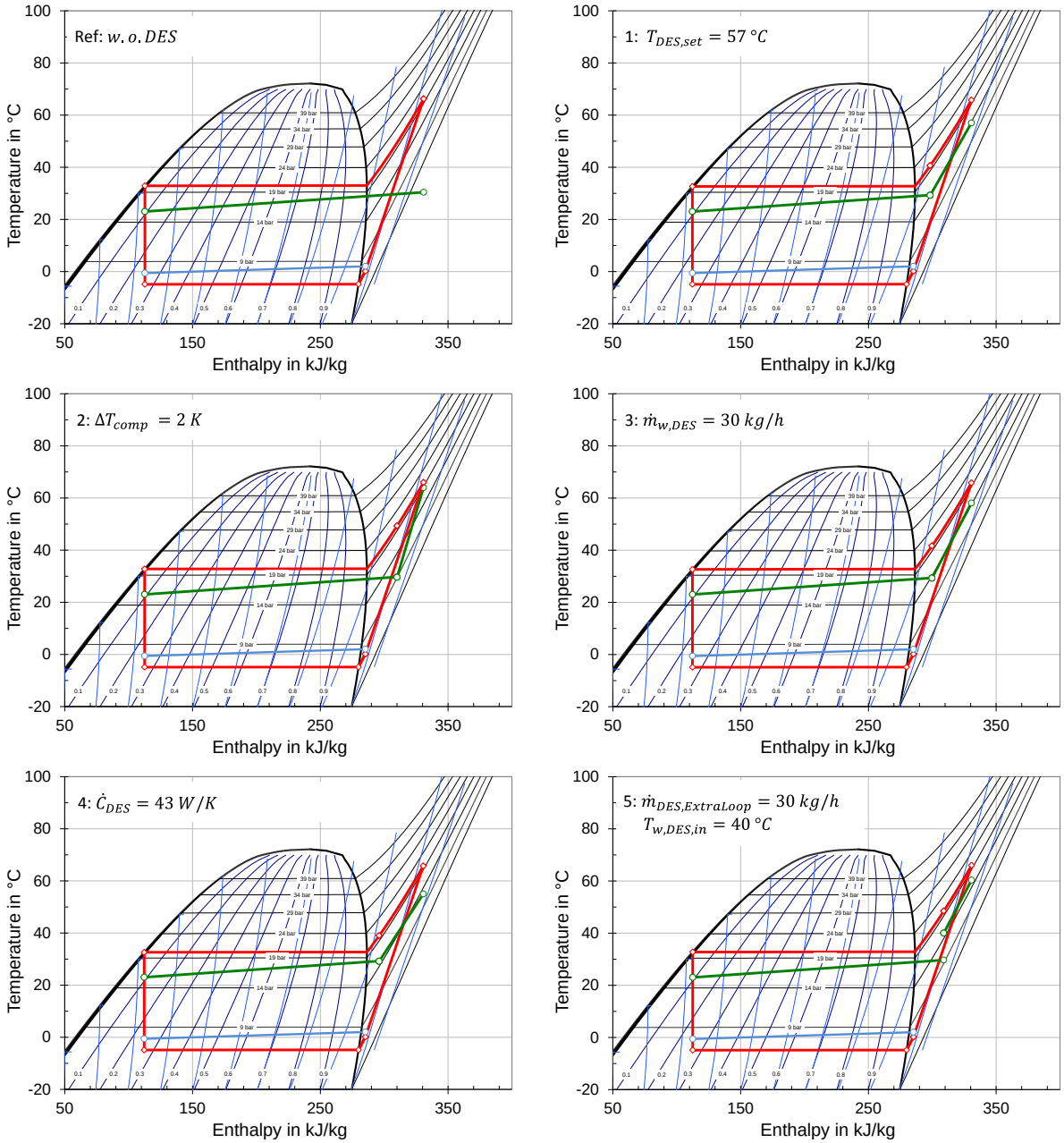

Figure 5: Steady state results of reference system (Ref) and strategy 1 to 5 at exemplary operating conditions (A2W30) in a temperature-enthalpy diagram for R410A

However, although the COP in the systems with DES is only slightly higher, the DES provides the benefit that water can be heated to a relatively high temperature at a low condensation temperature. This results in a higher annual system performance (SPF), which is investigated in the annual system simulations in the next section.

5.2 Annual system analysis

5.2.1 Reference system

Before analyzing the different strategies for the integration and control of the DES the results of the reference system are presented in Table 4. For the defined system, the climatic conditions of Graz and the SFH45 building the seasonal performance factor (SPF_{sys}) is 3.61, the electrical energy consumption of the whole system is 2603 kWh. Table 4 shows detailed results, especially for the heat pump system. Figure 6 shows the energy balance of the whole system with its inputs and outputs.

Table 4: Detailed results of the annual system simulation for the reference system

Parameter	Unit	Reference system
SPF_{sys}	-	3.61
$W_{el,sys}$	kWh_{el}	2603
No. of starts for DHW	-	287
No. of starts for SH	-	1225
Start losses	kWh_{th}	200
Heat losses Compressor	kWh_{th}	106
$W_{el,HP,DHW}$	kWh_{el}	770
$W_{el,HP,SH}$	kWh_{el}	1599
$Q_{HP,DHW\ only}$	kWh_{th}	1830
$Q_{HP,SH}$	kWh_{th}	4857
$Q_{HP,DHW\ DES}$	kWh_{th}	-
Penalty (SH)	%	0.1
Penalty (DHW)	%	0.3

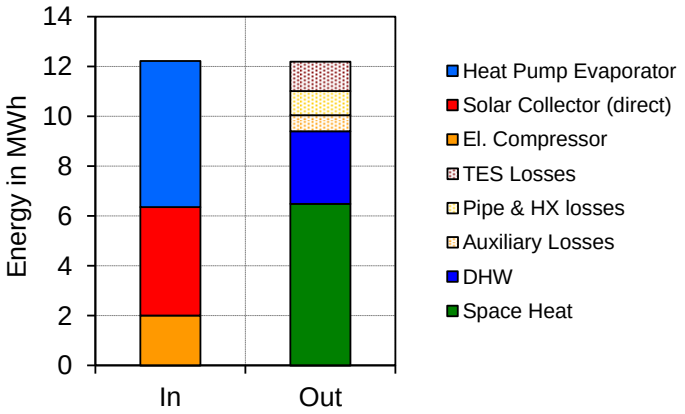

Figure 6: Energy balance for the reference system with all energy inputs into the system (left) and energy outputs (right)

5.2.2 Systems with DES

Figure 7 shows results obtained by annual system simulation for the different control and implementation strategies of the DES (strategy 1, 2, 3, 5), whereby a variation of a different parameter is done for each strategy. For strategy 4 this is not possible, the capacity flow is calculated depending on the operating conditions in every time step during the simulation.

The graphs in Figure 7 show the electrical energy savings compared to the reference system in percent on the ordinate and the changed parameter of the different strategies on the abscissa. For strategy 1 the DES outlet temperature is varied from 52 °C to 65 °C. The lowest value is chosen in order to prevent the system from switching to “direct” DHW preparation, which happens when T_{DHW} is lower than 48 °C. The highest value is set to 65 °C, because at higher set temperatures the results do not change significantly, which is due to the compressor discharge temperature, which is not significantly higher during a large part of the heating season.

The highest electrical energy savings with 4 % compared to the reference system and the highest increase of the SPF_{sys} of 4.2 % is achieved by a set temperature $T_{DES,set}$ of 57 °C. The temperature difference at the pinch point on the high pressure side is relatively low due to the high water mass flow rate (compare chapter 5.1) and on the other hand the TES inlet temperature at the top is relatively high. For $T_{DES,set}$ > 57 °C the temperature difference at the pinch point is increasing due to the lower mass flow rate. For $T_{DES,set}$ < 57 °C the energy input via DES into the TES is lower, so that the heat pump runs more in “direct” DHW preparation mode, which causes a lower efficiency.

The top right figure represents the results for strategy 2, in which the DES outlet temperature depends on the compressor discharge temperature. The highest electrical energy savings are obtained for a temperature difference of 9.5 to 10 K with about 3.9 %.

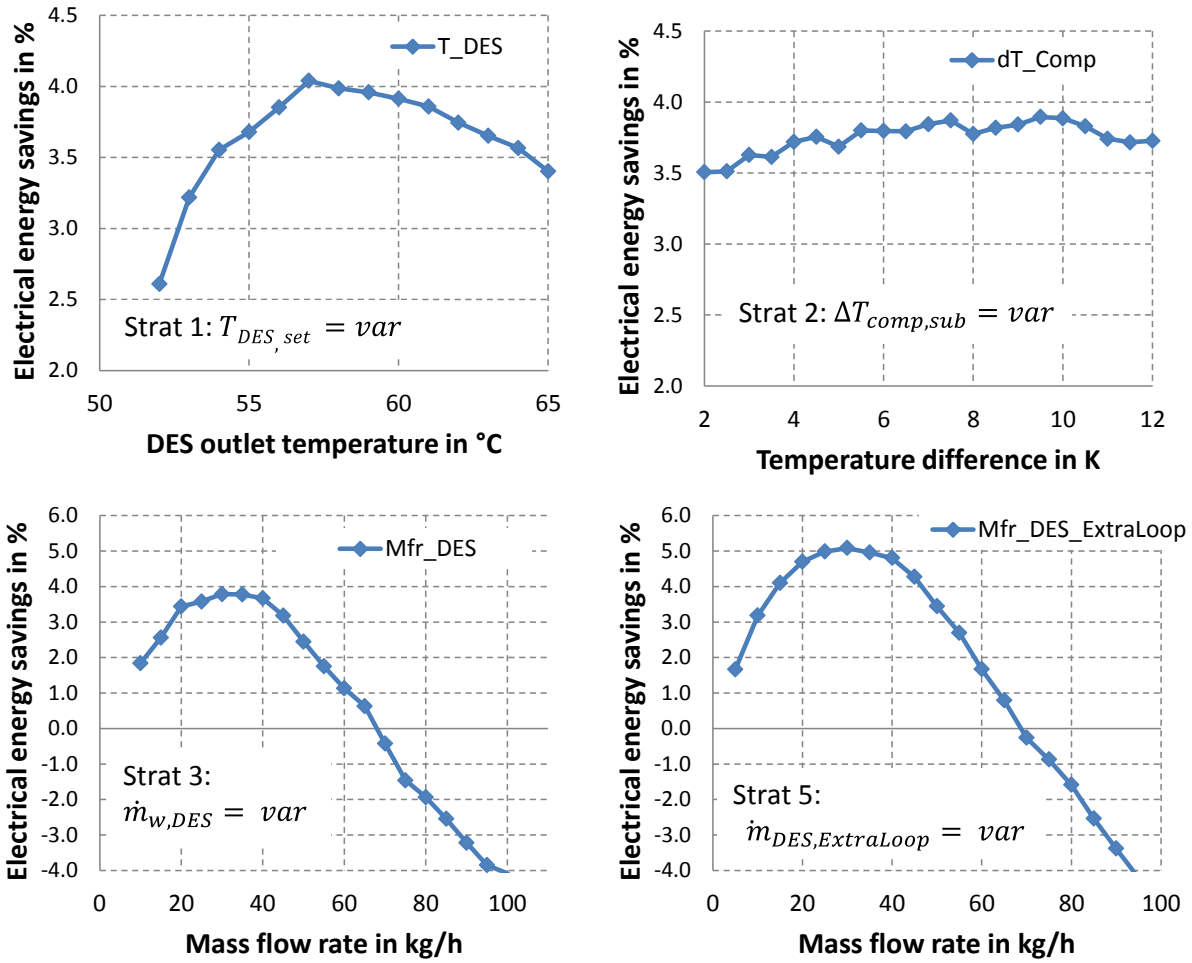

Figure 7: Annual system simulation results of the variation study for the strategies 1, 2, 3 and 5 by using different values for the parameters

For strategy 3 (bottom left in Figure 7), in which a fixed water flow rate through the DES $\dot{m}_{w,DES}$ is used, the highest electrical energy savings of 3.9 % are obtained for a flow rate of 30 to 35 kg/h. As discussed before this point represents a good compromise between the temperature difference in the pinch point and a high inlet temperature into the TES.

Strategy 4, in which the same capacity flow is used on the water and refrigerant side, shows a SPF improvement of 3.8 % and electrical energy savings of 3.8 % compared to the reference system.

The results for strategy 5 (bottom right of Figure 7) show qualitatively the same results as for strategy 3 but with higher electrical energy savings (5 % at about 30 kg/h), although an additional circulation pump for the DES loop is implemented. This is due to the lower heat losses of the connection pipes (210 kWh) compared to strategy 3 (301 kWh). Due to the reduced heat losses the “direct” DHW preparation can also be reduced from 871 kWh (for strategy 3) to 801 kWh.

For all strategies the improvement of SPF_{sys} as well as the electrical energy savings compared to the reference system is mainly due to the reduction of the “direct” DHW preparation.

5.2.3 Strategy 1 vs. reference system

Within this chapter it is discussed, why a system with DES yields a higher performance than a heat pump system without DES, by analyzing the results of strategy 1 and the reference system. The reason for analyzing strategy 1 is the simple integration (no extra loop), the simple control strategy, e.g. no calculation of capacity flow rates as discussed in strategy 4, and the good performance (compare Figure 7).

The results of the system simulations for the reference system show a seasonal performance factor SPF_{sys} of 3.61 and an annual electricity consumption $W_{el,sys}$ of 2603 kWh. With strategy 1

and an outlet temperature of 57 °C the SPF_{sys} can be increased by about 4.2 %, corresponding with electricity savings of about 4 % (compare Table 5). This is mainly due to simultaneous DHW preparation during space heating mode with higher temperatures by implementing a DES. The electrical energy consumption for direct DHW operation $W_{el,HP,DHW}$ can be reduced from 770 kWh for the reference system to 364 kWh for strategy 1. In addition, Figure 8 shows the energy balance of strategy 1 with its inputs (left) and outputs (right).

Another advantage of using a DES is that the total number of compressor starts (for DHW and SH) can be reduced, which should result in an extension of the compressor's life-time.

Table 5: Detailed results of the annual system simulation for strategy 1 and $\mathbf{t_{DES,set}}$ = 57 °C and changes compared to the reference system

Parameter		Strat. 1	Rel. Diff. to Ref.
SPF_{sys}		3.76	(+4.2 %)
$W_{el,sys}$	kWh_{el}	2498	(-4 %)
No. of starts for "direct" DHW		206	(-40 %)
No. of starts for SH		1161	(-5 %)
Start losses	kWh_{th}	193	(-4 %)
Heat losses Compressor	kWh_{th}	101	(-5 %)
$W_{el,HP,DHW}$	kWh_{el}	364	(-53 %)
$W_{el,HP,SH}$	kWh_{el}	1893	(+18 %)
$Q_{HP,DHW\ only}$	kWh_{th}	907	(-50 %)
$Q_{HP,SH}$	kWh_{th}	4964	(+2 %)
$Q_{HP,DHW\ DES}$	kWh_{th}	+1362	
Penalty (SH)	%	0.2	
Penalty (DHW)	%	0.3	

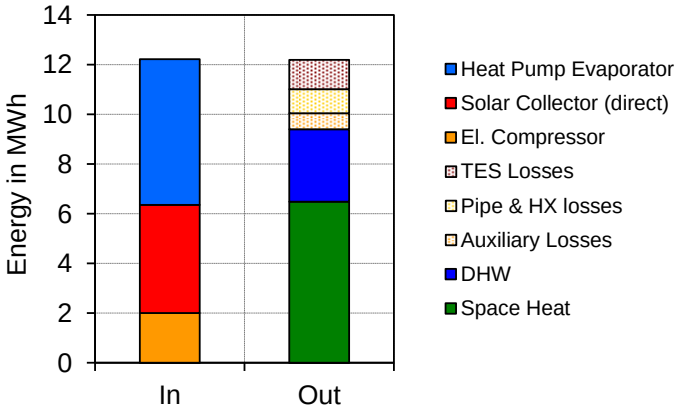

Figure 8: Energy balance of strategy 1 ($t_{DES,set}$ = 57 °C) with all energy inputs into the system (left) and energy outputs (right)

6 Conclusions

This paper deals with an extensive analysis of a DES applied in a combined solar and ASHP system for a residential low energy building (SFH45) under the central European climatic conditions of Graz. Within this article five different control strategies and types of implementation of a DES are studied.

For the investigations a validated heat pump model in TRNSYS is used. After defining the boundary conditions steady-state and annual simulations are carried out with the aim to analyze the energetic improvement by applying a DES. For the comparison between the reference system and the five strategies key figures are defined. In order to ensure the comfort level for the space heating and for DHW, penalty functions are implemented, which must not exceed 1 %.

The steady-state analysis of the different DES strategies at a typical operating condition during the heating season (A2W30) shows that there are only small differences of the COP. Strategy 4 shows the highest COP due to the lowest condensation temperature. Another finding is that the lowest pressure ratio (highest COP) is obtained in cases where the refrigerant outlet temperature of the DES is close to the saturated vapor line.

Annual system simulations for the considered combined solar and heat pump system with the five strategies are compared and analyzed. All strategies with DES result in a higher SPF_{sys} and a reduced annual electricity consumption $W_{el,sys}$. This is mainly due to the reduced amount of heat provided by the HP in direct DHW mode. Strategy five with an extra DES loop to the thermal energy storage yields the highest improvement of the SPF_{sys} (about 5.3 %) and shows the highest

savings in $W_{el,sys}$ (5 %) compared to the reference system. The improvement compared to the other DES strategies is mainly due to the lower heat losses of the connecting pipes because of the smaller dimension (inner diameter reduced from 25 mm to 8 mm), which leads to a higher reduction of the “direct” DHW preparation of the system, although an additional circulation pump is needed. However, strategy 1 to 4 also achieve electrical energy savings of about 4 %.

Lastly strategy 1 with the maximum electrical energy savings ($t_{DES,set} = 57\,°C$) of all investigated strategies is compared in detail with the reference system. On the overall system level electrical energy savings of about 4 % are achieved, the electricity consumption for “direct” DHW preparation are reduced by 53 %. Also a reduction of the total number of compressor starts is possible due to the DES, possibly enabling an extension of the compressor’s life-time.

Although this paper contains an extensive theoretical analysis of applying a DES in a heat pump system, some further questions can be raised. For instance investigations on air-source heat pumps with variable speed compressors could be performed in order to observe the improvements in case of a reduction of the compressor speed during partial load.

Reducing the pipe lengths between the DES and the TES would be advantageous, because the heat losses could be minimized. This is evident in the results of strategy 5, in which higher savings are achieved compared to the other strategies due to a reduced pipe diameter. A reduction of the pipe lengths would enable additional savings for all investigated strategies.

Furthermore the influence of the fraction of the DHW demand on the total heat demand and the influence of the flow temperatures of the space heating system could be studied in future work.

Acknowledgement

The research leading to these results has received funding from the European Commission under grant agreement nº 282825 – Acronym MacSheep.

References

[1] K.J. Chua, S.K. Chou , W.M. Yang, Advances in heat pump systems: a review, Applied Energy 87 (2010) 3611-3624.

[2] J. Heo, M.W. Jeong, C. Baek, Y. Kim, Comparison of the heating performance of air-source heat pumps using various types of refrigerant injection, International Journal of Refrigeration, 34 (2011) 444-453.

[3] T. Nowak, Heat pump market statistics report 2013, European Heat Pump Summit, Oct. 15 – 16, 2013, Nuremberg, Germany

[4] P. Biermayr , M. Eberl, R. Ehrig, H. Fechner, C. Kristöfel, K. Leonhartsberger, S. Martelli, C. Strasser, W. Weiss, M. Wörgetter, 2013. „Innovative Energietechnologien in Österreich Marktentwicklung 2012 – Biomasse, Photovoltaik, Solarthermie und Wärmepumpen“. Bundesministeriums für Verkehr, Innovation und Technologie, Report from R&D of Energy and Environment No. 17/2013, 2013, Austria

[5] A.H.W. Lee, J.W. Jones, Thermal performance of a residential desuperheater/water heater system, Energy Conversion and Management, 37(1996) 389–397.

[6] A.H.W. Lee, J.W. Jones, Analytical model of a residential desuperheater, Applied Energy, 57(1997) 271–285.

[7] S. Shao, W. Shi, X. Li, J. Ma, A new inverter heat pump operated all year round with domestic hot water. Energy Conversion and Management, 45 (2004) 2255–2268.

[8] P. Cui, H. Yang, J.D. Spitler, Z. Fang, Simulation of hybrid ground-coupled heat pump with domestic hot water heating systems using HVACSIM+. Energy and Buildings, 40 (2008) 1731–1736.

[9] A.L. Biaou, M.A. Bernier, Achieving total domestic hot water production with renewable energy. Building and Environment, 43 (2008) 651–660.

[10] B. Palm, Ammonia in low capacity refrigeration and heat pump systems. International Journal of Refrigeration, 31 (2008) 709–715.

[11] D. L. Blanco, K. Nagano, M. Morimoto, Steady state vapor compression refrigeration cycle simulation for a monovalent inverter-driven water-to-water heat pump with a desuperherater for low energy houses, International Journal of Refrigeration 35 (2012) 1833-1847

[12] D. L. Blanco, K. Nagano, M. Morimoto, Experimental study on a monovalent inverter-driven water-to-water heat pump with a desuperheater for low energy houses, Applied Thermal Engineering, 50 (2013) 826-836

[13] D. L. Blanco, K. Nagano, M. Morimoto, Impact of control schemes of a monovalent inverter-driven water-to-water heat pump with a desuperheater in continental and subtropical climates through simulation, Applied Energy 109 (2013) 374-386

[14] A. A. Safa, A. S. Fung, R. Kumar, Comparative thermal performances of a ground heat pump and a variable capacity air source heat pump system for sustainable houses, Applied Thermal Engineering 81 (2015) 279-287

[15] E. Entchev, L. Yang, M. Ghorab, E.J. Lee, Performance analysis of a hybrid renewable microgeneration system in load sharing applications, Applied Thermal Engineering 71 (2014) 697-704

[16] X. Liu, F. Hui, Q. Guo, Y. Zhang, T. Sun, Experimental study of a new multifunctional water source heat pump system, Energy and Buildings 111 (2016) 408-423

[17] A. Heinz, W. Lerch, R. Heimrath, heat pump condenser and desuperheater integrated into a storage tank: Model development and comparison with measurements, Applied Thermal Engineering 102 (2016) 465-475

[18] TRNSYS 17. “A transient system simulation program”, Version v17.01.0016, Solar Energy Laboratory, University of Wisconsin, Madison, 2012.

[19] R. Dott, T. Afjei, A. Dalibard, D. Carbonell, A. Heinz, M. Haller, A. Witzig, Models of Sub-components and Validation for the IEA SHC Task 44 / HPP Annex 38, Part C: Heat Pump Models, A technical report of Sub-task C, Deliverable C2.1 Part C, 2012.

[20] Emerson Climate Technologies, Copeland Selection Software v. 7.9, Compressor: ZH06K1P, http://www.emersonclimate.com/europe/en-

eu/Resources/Software_Tools/Pages/Download_Full_Instructions.aspx, 9th of March 2015

[21] F. Hengel, A. Heinz, R. Rieberer, ANALYSIS OF AN AIR SOURCE HEAT PUMP SYSTEM WITH SPEED CONTROLLED COMPRESSOR AND VAPOR INJECTION; Proceedings of 11th IEA Heat Pump Conference 12. – 16. May 2014, Montreal, Canada

[22] C. Bales, J. Betak, M. Broum, D. Chèze, G. Cuvillier, R. Haberl, B. Hafner, M. Y. Haller, Q. Hamp, A. Heinz, F. Hengel, A. Kruck, T. Matuska, I. Mojic, J. Petrak, S. Poppi, J. Sedlar, B. Sourek, B. Thissen, A. Weidinger, Optimized solar and heat pump systems, components and dimensioning, Deliverable 7.3, European Union Project-No. 282825 - Acronym "MacSheep", public document, 2014. http://macsheep.spf.ch/fileadmin/user_upload/macsheep/dokumente/MacSheep_D7-3_Simulations_M36_v150618_Final_revised.pdf, 27th of July 2015

[23] M. Haller, B. Perers, C. Bales, J. Paavilainen, A. Dalibard, S. Fischer, E. Bertram, TRNSYS Type 832v3.10 "Dynamic Collector Model by Bengt Perers", Updated Input-Output Reference, 2012.

[24] H. Drück, MULTIPORT Store-Model for TRNSYS, Type 340 version 1.99F, 2006, http://www.trnsys.de/download/de/ts_type_340_de.pdf, 27th of July 2015

[25] Transsolar Energietechnik GmbH, Type 56 Multizone Building modeling with Type 56 and TRNBuild, TRANSSOLAR Energietechnik GmbH, Stuttgart, Germany, 2010.

[26] R. Dott, M. Haller, J. Ruschenburg, F. Ochs, J. Bony, IEA-SHC Task 44 Subtask C technical report: The Reference Framework for System Simulations of the IEA SHC Task 44 / HPP Annex 38: Part B: Buildings and Space Heat Load, IEA-SHC, 2013, http://www.taskx.iea-shc.org/data/sites/1/publications/T44A38_Rep_C1_B_ReferenceBuildingDescription_Final_Revised_130906.pdf, 27th of July 2015

[27] M. Haller, Intercomparison of System Simulation Results for the IEA SHC Task 44 / HPP Annex 38, A technical report of subtask C, Deliverable C4.1, 15th April 2013